

Indirect Cutting Force Measurement and Cutting Force Regulation Using Spindle Motor Current

Gi D. Kim*

Won T. Kwon**

Chong N. Chu***

*Research Scientist Gi-dae Kim, School of Mechanical and Aerospace Engineering, Seoul National University, Seoul 151-742, Korea. Tel: +82-2-880-1678 Fax: +82-2-880-7259

E-mail : gidkim@plaza.snu.ac.kr

**Assistant Professor Won-tae Kwon, Department of Mechanical Engineering, University of Seoul, Seoul 130-743, Korea. Tel: +82-2-2210-240 Fax: +82-2-2248-5110

E-mail : kwon@uoscc.uos.ac.kr

***Associate Professor Chong-nam Chu, School of Mechanical and Aerospace Engineering, Seoul National University, Seoul 151-742, Korea. Tel: +82-2-880-7136 Fax: +82-2-875-2674

E-mail : cnchu@plaza.snu.ac.kr

ABSTRACT

Quasi-static cutting force variation in milling process was measured indirectly using spindle motor current. Quasi-static sensitivity of the spindle motor current is higher at higher spindle speed range. The spindle motor current is independent of feed direction. The linear relationship between the cutting force and the spindle motor RMS current at various spindle rotational speeds was obtained. Frequency to voltage (F/V) converter voltage was measured to identify the spindle speed and to determine the cutting force at various spindle speeds. Based on these measurements, cutting force was regulated at a constant level by feedrate control. Practicability of the cutting force regulation system using spindle motor current was shown by

implementation to an FMS.

Keywords: Spindle motor RMS current, Quasi-static sensitivity, F/V converter,

Cutting force regulation, Feedrate control

LIST OF FIGURES

Fig. 1: Cutting force model.

Fig. 2: Bode plot of current hall effect sensor.

Fig. 3: Quasi-static sensitivities of the feed and spindle drive systems.

(a) Feed drive system

(b) Spindle drive system

Fig. 4: Relationship between the spindle rotational speed and the voltage measured from F/V converter

Fig. 5: Cutting force and spindle motor current vs. feedrate.

(Machine: MCH-10, DOC: 3 mm, Spindle speed: 1,000 rpm,

Tool: carbide flat endmill, 2 teeth, Diameter = 20 mm, Workpiece: SM45C)

(a) Cutting force vs. feedrate

(b) Spindle motor current vs. feedrate

Fig. 6: Spindle motor current vs. cutting force.

(Machine: MCH-10, DOC: 3 mm, Spindle speed: 1,000 rpm,

Tool: carbide flat endmill, 2 teeth, Diameter = 20 mm, Workpiece: SM45C)

(a) In high gear ratio

(b) In low gear ratio

Fig. 7: Experiments at various cutting speeds in TCH-80 machining center.

(Machine: TCH-80, Gear change: 1400 rpm, DOC: 0 mm ~ 5 mm,

Feedrate: 200 mm/min, Tool: HSS flat endmill, 4 teeth, Diameter = 25 mm,

Workpiece: GC30)

Fig. 8: Experimental set-up for feedrate control.

Fig. 9: Flowchart of feedrate control.

Fig. 10: Cutting force regulation pattern according to the proportional gain (K_p).

Fig. 11: Taper machining of composite material (DOC: 1 mm ~ 4 mm, 600 rpm).

- a. Feedrate fixed (160 mm/min)
- b. Feedrate controlled

Fig. 12: Workpiece shape and tool path for circular machining.

Fig. 13: Circular taper machining (DOC: 2 mm ~ 5 mm, 3000 rpm).

- a. Feedrate fixed (170 mm/min)
- b. Feedrate controlled

NOMENCLATURES

F_T : Tangential force acting on the tool.

F_R : Radial force acting on the tool.

K_T : Specific cutting pressure.

a : Axial depth of cut.

$h(\bullet)$: Instantaneous uncut chip thickness.

$\bullet \bullet \bullet$: Angular position of the tooth.

S_f : Feed per tooth.

r_f : Ratio of radial force to tangential force.

R : Cutter radius.

T_c : Cutting torque.

T_{c_max} : Peak cutting torque per revolution.

F_{c_max} : Peak cutting force per revolution.

I_{rms} : RMS (root mean square) value of AC motor current.

I_f : Feed motor current.

I_s : Spindle motor current.

F_x : Feed force.

DOC: Depth of cut.

K_p : Proportional gain.

1. Introduction

Machine tool operator needs to monitor an abrupt malfunction during machining, such as overload on the tool, tool failure, machine tool chatter, etc. Many researches have been carried out to monitor and diagnose the malfunctions during machining. Cutting force signals, AE signals, and acceleration signals have been used to monitor the cutting process [1-6]. It is known that cutting process is well identified from cutting force signals measured by a tool dynamometer. A tool dynamometer is, however, impractical to use in industrial environments. Other sensors such as an AE sensor and an accelerometer are sensitive to noise and show different results according to the attached position. Furthermore, they may interfere with normal machining operation.

Motor current can be used to measure the cutting force. Motor current is proportional to the output torque of the motor and therefore the cutting force. Thus, current measurement sensor can be used to monitor the cutting process in a manner similar to a tool dynamometer. Because current measuring sensor is physically remote from the restrictive and harsh cutting site, it is more durable, more flexible, and less expensive than a tool dynamometer. Stein et al. estimated cutting force and cutting torque using DC and AC servo motor currents [7-8]. Park and Settineri monitored cutting process using spindle motor power [9]. Altintas et al. used AR(1) model to detect tool breakage using feed motor current signal [10]. Lee et al. detected tool breakage using advanced AR(1) model of the feed motor current [11]. Liu et al. monitored drill fracture using 3-phase induction motor current [12].

During milling process, especially during rough machining, overload on the tool can lead to tool fracture or machine tool chatter, and damage the workpiece and machine tool itself. Therefore, feedrate is usually set to a low level to avoid the overload. Sometimes, operators manually decrease the feedrate under severe cutting condition and increase it under light cutting condition. Hence, it is necessary to detect the overload on the tool and to regulate the cutting force at a constant level during machining in order to increase productivity. In this paper, cutting force was measured indirectly from spindle motor current of horizontal machining centers. It is difficult to use the feed motor current for monitoring multi-axis machining because of different phase lags of each axis. On the other hand, spindle motor current is independent of the cutting direction. After the cutting force was measured from the spindle motor current, it was regulated at a constant level by feedrate control. The cutting force regulation system was implemented to an actual FMS.

2. Cutting torque, cutting force, and spindle RMS current

Cutting torque can be calculated from the cutting force model as shown in Fig. 1. The cutting force can be described as a function of cutting pressure acting on the instantaneous uncut chip area [13].

$$F_T = K_T a h(\phi) = K_T a S_c \sin \phi \quad (1)$$

$$F_R = r_1 F_T \quad (2)$$

where \square and \square are tangential and radial forces acting on the tool; \square is specific cutting pressure; a is axial depth of cut;

$h(\phi)$ is instantaneous uncut chip thickness; S_f is feed per tooth; ϕ is angular position of the tooth; and λ is the ratio of radial force to tangential force. Cutting torque, T_c , is calculated from the tangential force and the cutter radius, R .

$$T_c = R * F_T(3)$$

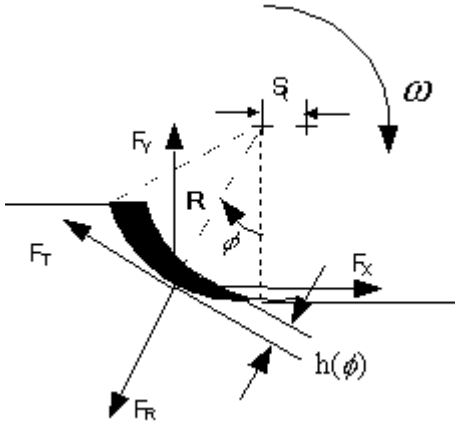


Fig. 1: Cutting force model.

Peak cutting torque per tooth occurs when the uncut chip thickness ($h(\phi)$) is maximum. For full immersion cutting with four or less teeth per tool, the peak cutting torque is the y directional cutting force measured by a tool dynamometer multiplied by the cutter radius when angular position of the tool is 90° .

$$T_{c_max} = R * F_Y(at \phi = 90^\circ) (4)$$

Also, the peak cutting force per tooth for full immersion cutting is

$$\begin{aligned}
 F_{C_max} &= \sqrt{(F_X^2 + F_Y^2)}_{max} = \sqrt{(F_T^2 + F_R^2)}_{max} \\
 &= \sqrt{1 + \lambda^2} * F_T_{max} = \sqrt{1 + \lambda^2} * F_Y_{max} \quad (5)
 \end{aligned}$$

(b) Spindle drive system

Fig. 2: Bode plot of current hall effect sensor.

From Eq. 4 and Eq. 5, the peak cutting force per tooth is proportional to the peak cutting torque.

$$F_{c_max} = \frac{\sqrt{1 + f_1^2}}{R} * T_{c_max} \quad (6)$$

RMS (root mean square) value of AC motor current is equivalent to the DC current, which is proportional to the motor torque.

$$I_{rms} = \sqrt{\frac{I_u^2 + I_v^2 + I_w^2}{3}} \quad (7)$$

3. Characterization of spindle motor current

Machine tools used in this work are horizontal machining centers (model : MCH-10 and TCH-80, manufactured by TONG-IL Heavy Industry Co.). Permanent magnet synchronous motors are used for x and y direction feed drives and a squirrel-cage induction motor is used for the spindle drive. The spindle motor and the feed motor currents were measured by current hall effect sensors and the cutting force was measured by a tool dynamometer. Measured data were stored in the computer through AD2200 AD converter. The relationship between the spindle motor current and the cutting force was obtained from the stored data.

When periodic cutting force is estimated by measuring the motor current, the bandwidth of the hall sensor must be higher than the frequency of the applied cutting force, i.e., the tooth passing frequency. Preliminary experiments were carried out to determine the bandwidth of the hall sensor as shown in Fig. 2.

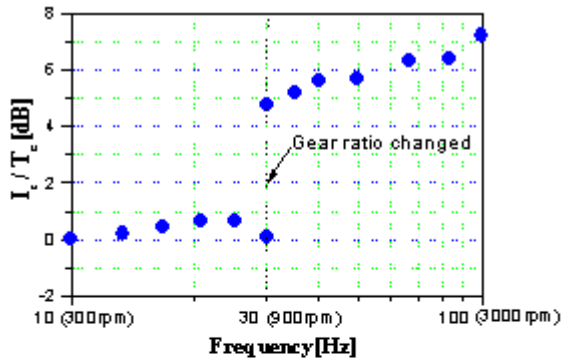
It is shown that the current hall sensor signal will not be distorted up to the tooth passing frequency of 1 kHz. To eliminate high frequency noise, the motor current was measured through an analog filter with 50 Hz cut-off frequency for the feed motor and 260 Hz for the spindle motor.

Generally, it is known that the bandwidth of the feed drive system is about 40 Hz and the bandwidth of the spindle drive system is lower than 5 Hz [14]. Bandwidth of the system is important to measure the dynamic activities of the machine tool, such as tool breakage and chatter. However, for cutting force regulation, only peak cutting force is needed. To define the quasi-static sensitivity of the feed drive system, the ratio of the peak RMS feed motor current (I_p) to the peak feed force (F_x) per revolution was calculated. Similarly, to define the quasi-static sensitivity of the spindle drive system, the ratio of the peak RMS spindle motor current (I_s) to the peak cutting torque (T_c) per revolution was calculated.
$$= \frac{1}{Rev} \sum_{i=1}^{Rev} \frac{\max(I_{rms})_s[i]}{\max(T_c)[i]} \quad (\text{where,}$$

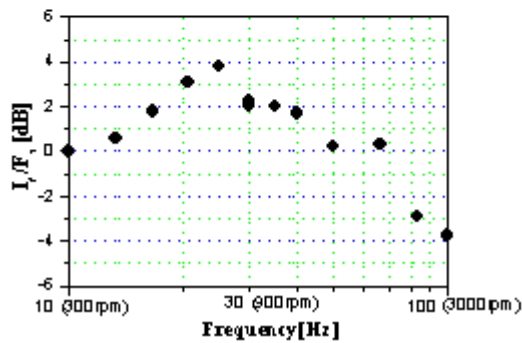
Rev is No. of tool revolutions)

Quasi-static sensitivity

Figure 3 shows the change of the quasi-static sensitivities of the feed and spindle drive systems as the spindle speed increases. To minimize the noise effect, moving averaged data were used. Each point represents the average of the ratio between the current and the feed force or cutting torque as the spindle rotational speed increases from 300 rpm to 3000 rpm. In these experiments, the feed per tooth was fixed at 0.15 mm/min and depth of cut was 4 mm during machining with a carbide flat endmill having 2 flutes. As the spindle speed increases, the quasi-static sensitivity of the feed drive system decreases, while that of the spindle drive system increases.



(a) Feed drive system



(b) Spindle drive system

Figure 3

The machining center used in this research changes the spindle gear ratio at 900 rpm from high gear ratio (1:4.81) to low gear ratio (1:1.157). Because of the effect of the different gear coupling on the motor torque, the quasi-static sensitivity of the spindle drive system shows discontinuity at 900 rpm.

A major disadvantage of using the motor current in estimating cutting force is that the relationship between the motor current and the static cutting force changes as the spindle rotational speed changes. To overcome this problem, Frequency to voltage (F/V) converter voltage proportional to the spindle rotational speed was measured as shown in Fig. 4.

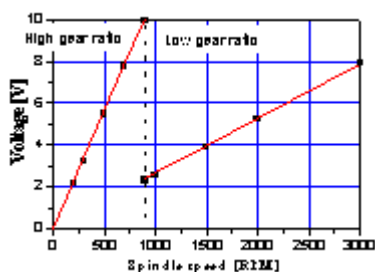
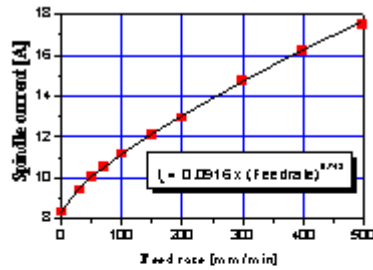


Fig. 4: Relationship between the spindle rotational speed and the voltage measured from F/V converter.

At each gear ratio, the voltage measured by the F/V converter is shown to be proportional to the spindle speed. From the measured voltage, the spindle rotational speed can be identified.

From the preliminary experiments, the relationship between the peak cutting force and the spindle RMS current per revolution was obtained under various cutting conditions. Figure 5 shows the variations of the peak cutting force and spindle RMS current as the feedrate changes from 30 mm/min to 500 mm/min. The spindle speed was fixed at 1,000 rpm. When the feedrate is low, size effect causes nonlinearity [15]. The spindle RMS current shows the same behavior as shown in Fig. 5.



(a) Spindle motor current vs. feedrate

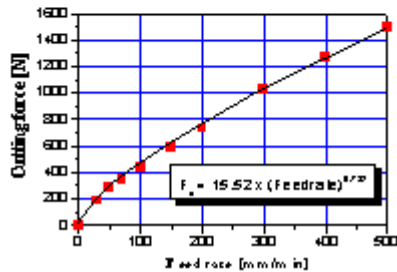


Fig.5: Cutting force and spindle motor current vs. Feedrate (Machine:MCH-10,DOC:3 mm, Spindle speed:1,000 rpm, Tool: carbide flat endmill, 2 teeth, Diameter?= 20 mm, Workpiece: SM45C).

The linear relationship between the cutting force and the spindle RMS current was obtained regardless of the feedrate as shown in Fig. 6.

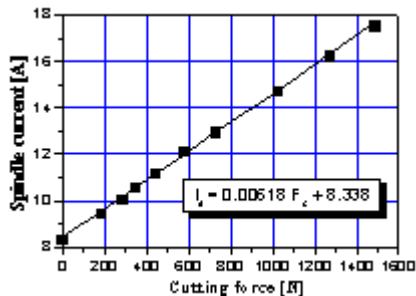


Fig. 6: Spindle motor current vs. cutting force

(Machine: MCH-10, DOC: 3 mm, Spindle speed: 1,000 rpm,

Tool: carbide flat endmill, 2 teeth, Diameter?= 20 mm,

Workpiece: SM45C).

To obtain a more reliable relationship between the peak cutting force and the spindle RMS current, other experiments were performed with a different machining center under different cutting conditions. The results are shown in Fig. 7. As depth of cut increases with fixed feedrate, the peak cutting force and the spindle RMS current increased linearly. As the spindle speed changes, the linear relationship between the cutting force and the spindle RMS current changed.

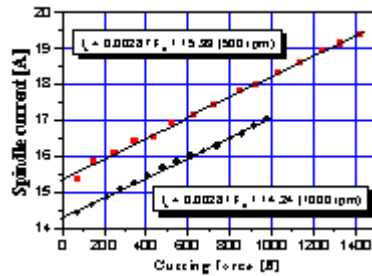


Fig. 7 Experiments at various cutting speeds in TCH-80 machining center (Machine: TCH-80, Gear change: 1400 rpm, DOC: 0 mm ~ 5 mm, Feedrate: 200 mm/min, Tool: HSS flat endmill, 4 teeth, Diameter = 25 mm, Workpiece: GC30).

8. Feedrate control

Figure 8 shows the configuration of the feedrate control system. Programmable machine controller program was modified so that the computer and the DSP board can control the feedrate. The DIO port on the TMS320C32 DSP board was used to control the feedrate override percentage ranging from 0% to 255%. Current hall effect sensors measured U and V phase currents of the spindle motor.

By measuring the F/V converter voltage of the spindle and by obtaining the linear relationship between the cutting force and the spindle RMS current from the preliminary experiments, cutting force could be estimated regardless of the cutting condition.

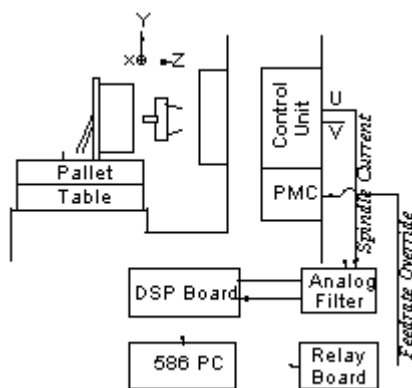


Fig. 8: Experimental set-up for feed-rate control

Flowchart of the feedrate control system is shown in Fig. 9 (at the end of this paper).

DSP board was used to process the measured current and perform following calculations. Firstly, the RMS spindle motor current is obtained and compared with the maximum and minimum threshold determined in preliminary experiments. If the value is larger than the maximum threshold or smaller than the minimum threshold, the difference between the measured current and the threshold is calculated. Then, the feedrate is decreased by the amount proportional to the difference when the spindle RMS current is larger than the maximum threshold. The feedrate is increased when the spindle RMS current is smaller than the minimum threshold. When the feedrate is controlled proportionally, the maximum-to-minimum threshold gap and the magnitude of proportional gain (K_p) are determined by trial and error through preliminary experiments. When the maximum-to-minimum threshold gap is smaller than the current noise or when the proportional gain is large, the control system tends to be unstable and the cutting force diverges. When the maximum-to-minimum threshold gap is large or the proportional gain is small, the system is stable but the cutting force is not regulated at a constant level. The effect of the feedrate control on surface roughness was neglected in this study, because prevention of overload on the tool and reduction of cutting time is more important during rough machining.

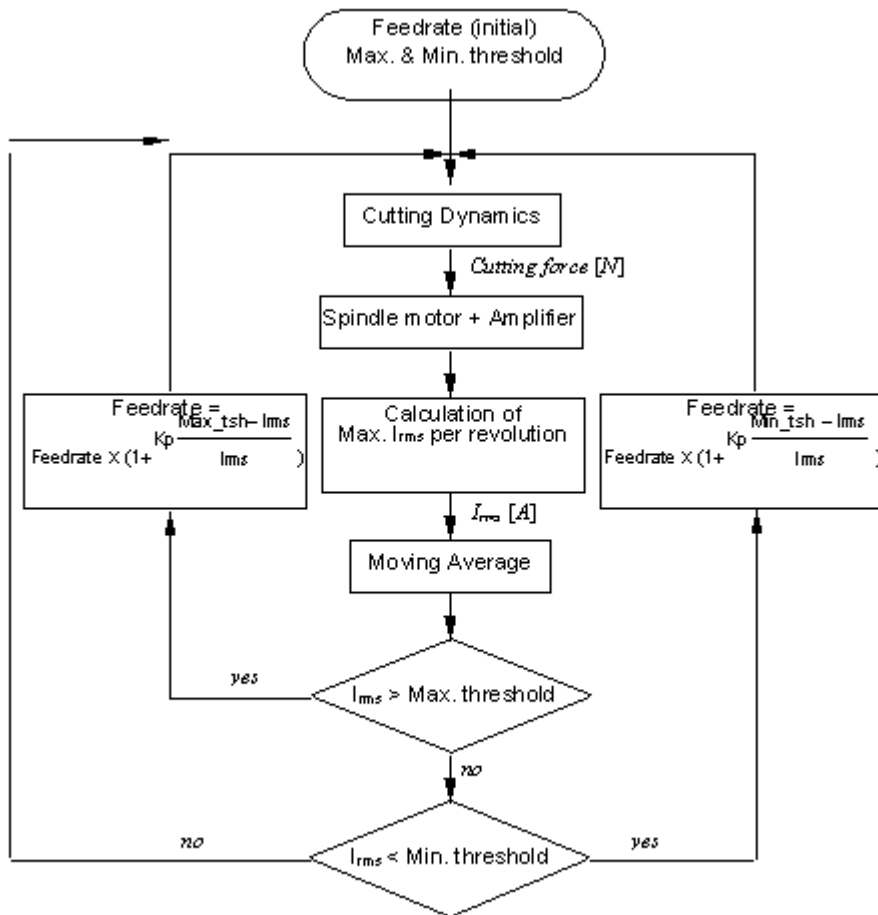


Fig 9 Flowchart of Feed control system

The effect of the proportional gain on the regulation of cutting force and spindle motor current is shown in Fig. 10. In this experiment, the depth of cut increased from 1 mm to 5 mm by 1 mm increment. The tool was carbide flat endmill and the workpiece material was SM45C. When the depth of cut reached 3 mm, the spindle motor current became larger than the maximum threshold and the feedrate control was initiated. The proportional gain and the maximum-to-minimum threshold gap was set to 0.5 and 0.4 A, respectively. Sudden increment of the cutting force at the entrance or at the step was unavoidable.

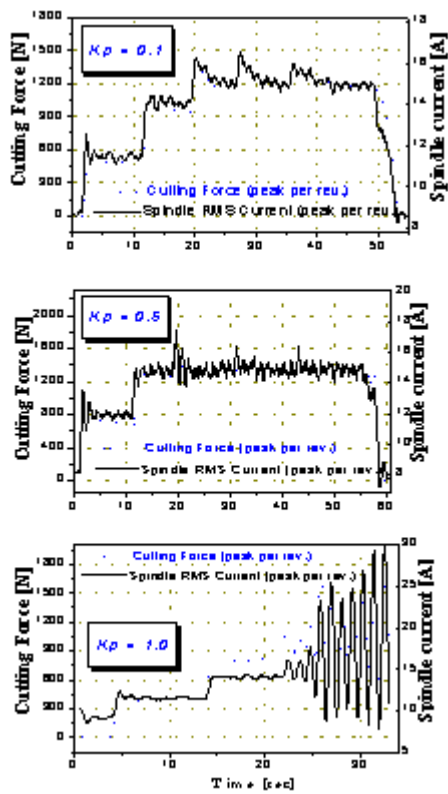


Fig. 10: Cutting force regulation pattern according to the proportional gain (K_p).

Figure 11 (a) shows the cutting force and spindle current variations when the workpiece material changed from SM45C to Aluminum during machining. The depth of cut was increased gradually from 1 mm to 4 mm while the spindle speed was set to 600 rpm. As can be seen in Fig. 11 (b), the cutting force was regulated at a constant level.

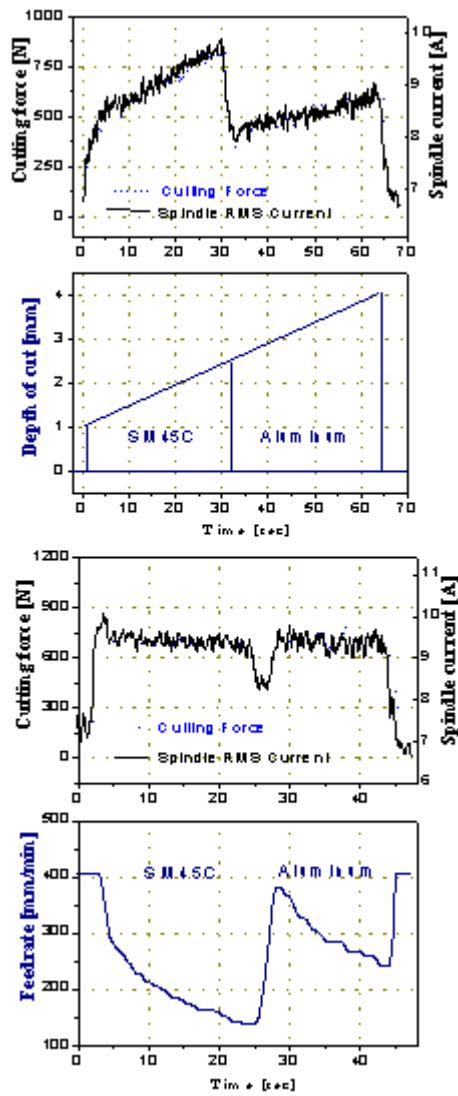


Fig. 11: Taper machining of composite material

(DOC: 1 mm ~ 4 mm, 600 rpm)

Figure 12 shows the workpiece shape and the tool path for circular taper machining. The tool moved from A to B in linear motion. The depth of cut was 2 mm in the linear motion and the spindle speed was 3000 rpm. Then, the tool moved to C in circular motion with the depth of cut gradually increasing from 2 mm to 5 mm. It returned to B with the depth of cut gradually decreasing from 5 mm to 2 mm.

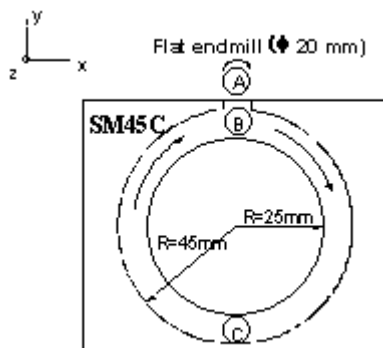
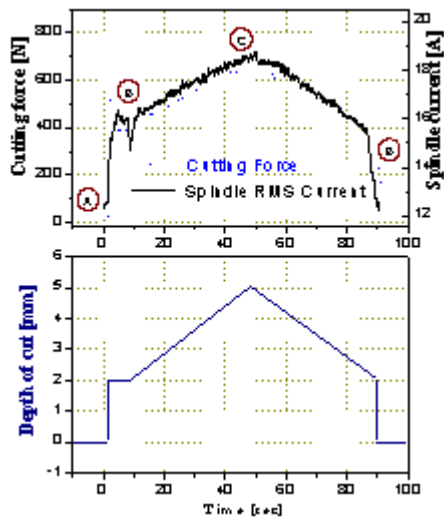


Fig. 12: Workpiece shape and tool path for circular machining

Figure 13 shows the variation of the cutting force, the spindle RMS current and the controlled feedrate during the circular taper machining. It is shown that even in multi-axis machining at high spindle rotational speed, the cutting force can be estimated and regulated reliably using the spindle motor current. It should be noted from Fig. 13 (a) that spindle current decreased suddenly at region B due to feed motor deceleration. Because of the sudden decrease of spindle current, feedrate increased suddenly when feedrate is controlled as shown in Fig. 13 (b).



(a) Feedrate fixed (170 mm/min)

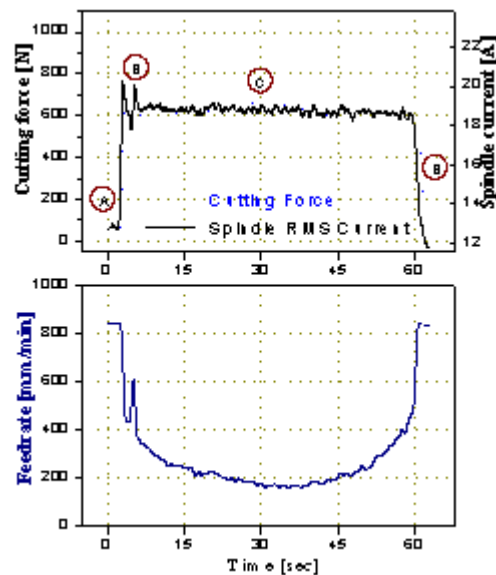


Fig. 13: Circular taper machining (DOC: 2 mm ~ 5 mm, 3000 rpm).

In case that the spindle motor starts or accelerates, large current flows into the spindle motor. The large current induced during acceleration should be distinguished from the large spindle current due to overload on the tool. In this research, large current is neglected if it is within 3 seconds after the spindle motor starts to rotate.

Presented method was successfully implemented to a machining center in an FMS in the industry. The DSP board has its own CPU and is used to receive current signals and to control the feedrate. It not only allows on-line control but also avoids conflict between the machine control computer and the main computer in FMS center during communication.

5. Conclusions

1. Spindle motor current was used to measure the cutting force indirectly. RMS value of 3 phase currents was shown to be proportional to the cutting force.
1. Quasi-static sensitivity of the spindle motor current to cutting force is higher in high spindle speed range. Spindle motor current also has an advantage to estimate the cutting force over feed motor current during multi-axis motion such as circular motion.
2. The ratio of the linearity between the cutting force and the spindle motor current varies as the cutting speed changes. Frequency to voltage (F/V) converter voltage was measured to identify the spindle speed and to determine the linear relationship between the spindle motor current and cutting force at various rotational speeds.
3. The cutting force was regulated at a constant level by feedrate control. When the cutting force is regulated, the spindle RMS current remains between the maximum and minimum threshold determined in the preliminary experiments at various spindle rotational speeds.
4. Presented method was implemented to a machining center of an actual FMS. DSP board was used to import current signals from the machining center and to control feedrate by sending override signals to the machine tool controller.

REFERENCES

1. J. Tlustý, Y. S. Tarn. Sensing Cutter Breakage in Milling. *Annals of the CIRP* 1988; 37: 45-51.
2. Y. Altintas, I. Yellowley, J. Tlustý. The Detection of Tool Breakage in Milling Operations. *ASME Journal of Engineering for Industry* 1988; 110: 271-277.
3. Y. Altintas. In-process Detection of Tool Breakages using Time Series Monitoring of Cutting Forces. *Int. J. Mach. Tools Manufact.* 1988; 28(2): 157-172.
4. Y. Altintas, I. Yellowley. In-process Detection of Tool Failure in Milling using Cutting Force Models. *ASME Journal of Engineering for Industry* 1989; 111: 149-157.
5. D. Yan, T. I. El-Wardany, M. A. Elbestawi. A Multi-Sensor Strategy for Tool Failure Detection in Milling. *Int. J. Mach. Tools Manufact* 1995; 35(3): 383-398.
6. S. C. Lin, M. R. Hu. Low Vibration Control System in Turning. *Int. J. Mach. Tools Manufact.* 1992; 32(5): 629-640.
7. J. L. Stein, D. Colvin, G. Clever, C. H. Wang. Evaluation of DC Servo Machine Tool Feed Drives as Force Sensors. *ASME Journal of Dynamic Systems Measurement and Control* 1986; 108: 279-288.
8. J. L. Stein, C. H. Wang. Analysis of Power Monitoring on AC Induction Drive Systems. *ASME Journal of Dynamic Systems Measurement and Control* 1990; 112: 239-248.
9. J. J. Park, L. Settineri. Cutting Torque Estimation Using Spindle Power Measurements. *Transactions of NAMRI of SME* 1994; 24: 85-90.
10. Y. Altintas. Prediction of Cutting Forces and Tool Breakage in Milling from Feed Drive Current Measurements. *ASME Journal of Engineering for Industry* 1992; 114: 386-391.
11. J. M. Lee, D. K. Choi, J. Kim, C. N. Chu. Real-Time Tool Breakage Monitoring for NC Milling Process. *Annals of the CIRP* 1995; 44: 59-62.
12. H. S. Liu, B. Y. Lee, Y. S. Tarn. Monitoring of Drill Fracture from the Current Measurement of a Three-Phase Induction Motor. *Int. J. Mach. Tools Manufact.* 1996; 36(6): 729-738.
13. M. E. Martelotti. Analysis of the Milling Process. *ASME Journal of Engineering for Industry* 1941; 63: 667.
14. K. Matsushima, P. Bertok, T. Sata. In-Process Detection of Tool Breakage by Monitoring Spindle Motor Current of a Machine Tool. *Measurement and Control for Batch Manufacturing, The Winter Annual Meeting of ASME* 1982: 14-19.
15. W. A. Kline, R. E. DeVor, J. R. Lindberg. The Prediction of Cutting Forces in End Milling with Application to Cornering Cuts. *Int. J. Mach. Tool Des. Res.* 1982; 22(1):7-2